Journal of Sound and Vibration (1990) **139**(2), 277–287

DAMPING AND VIBRATION CONTROL OF UNIDIRECTIONAL COMPOSITE LAMINATES USING ADD-ON VISCOELASTIC MATERIALS

C. T. Sun, B. V. Sankar and V. S. Rao

Department of Aerospace Engineering, Mechanics and Engineering Science, University of Florida, Gainesville, Florida 32611, *U.S.A.*

(*Received* 23 *August* 1988, *and in revised form* 15 *August* 1989)

This paper describes the development of an efficient finite element model for dynamic analysis of laminated beams treated by a constrained viscoelastic layer. The finite element model is designed so as to represent the viscoelastic core shear accurately. An offset-beam element which takes shear deformation into account and is specially suited for modeling such laminated beams is developed. The laminated beam and constraining layer are modeled by using the offset beam element. The viscoelastic core is modeled by using plane finite elements which are compatible with the beam elements. System damping and tip displacement are computed and compared with those measured experimentally by using the impulse-frequency response technique. Results show that dynamic response is improved by use of such damping treatments.

1. INTRODUCTION

The potential for the use of constrained viscoelastic layers in numerous dynamic applications has motivated the authors to develop an accurate and efficient method to estimate damping in such structures [1]. Considerable work has been done in the past few years to analyze constrained viscoelastic layer damping. Early work in the field can be found in the work of Ross, Ungar and Kerwin [2]. Plunkett and Lee discussed the optimization of constrained viscoelastic layer damping for beams [3]. They assumed in their analysis that the treatment is always symmetric and that the base structure is perfectly elastic. While this is reasonable for metals, fiber-reinforced plastics are known to have much higher loss factors. Results from this work show that consideration of the loss factor of the base structure is essential for accurate modelling of high-damping composites.

More recently, finite element techniques have been used to address this problem [4–6]. Most of the work done so far is on damping treatment applied to metals. Advanced fiber-reinforced composites are prime candidates for several interesting applications where damping is a key parameter. Improvement of damping characteristics of these materials makes them even more attractive. Since most composite structural elements in military and space applications are subject to severe dynamic loads, additional vibration control becomes necessary. This can be achieved by using damping treatments.

High damping in a structure can often improve performance in a dynamic load environment. Efficient methods for predicting damping in a structure are required, so that means of increasing damping by design can be explored. Johnson *et al.* and Brockman have discussed some of the finite element modeling techniques that are currently popular for modeling structures containing viscoelastic materials [7, 8].

0022-460X/90/110277+11 $03.00/0

Much of the problems in analyzing damping in structures is due to complicated geometries; it is therefore natural to look to finite element solutions. The method considered here makes use of the correspondence principle of viscoelasticity. When applied stresses are not too large, the composite and its constituent materials exhibit linear viscoelastic behavior. For such materials, due to the correspondence principle, the Young's modulus and shear modulus can be treated as complex quantities. The real part is called the storage modulus and the imaginary part the loss modulus.

The direct frequency response technique [7] was used for the analytical estimation of damping and tip displacement. Experimental measurement of damping was done by using the impulse-frequency response technique. In composite base structures, several factors influence system response. For example, the stacking sequence in the base structure, and the location, amount and type of treatment influence the response strongly. The influence of some of the parameters is presented here.

2. FINITE ELEMENT ANALYSIS

The finite element method was used to evaluate damping in the structure for different lengths of treatment of the constrained viscoelastic layer. The arrangement used for modeling the three layer sandwich is shown in Figure 1.

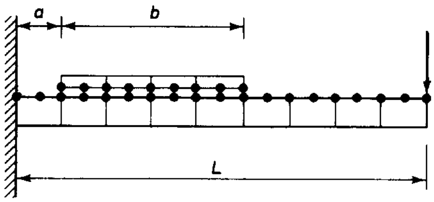

Figure 1. Typical finite element mesh.

The base structure and constraining layer were modeled by using a specially developed *three-node*, seven-degree-of-freedom, offset beam element. The element is shear-deformable, which is significant for fiber-reinforced composites. A key feature of this element is its ability to account for coupling between stretching and bending deformations. This allows for the beam nodes to be offset to one surface of the beam, coincident with the nodes of the adjoining element. The viscoelastic core is modeled by using a rectangular plane stress element that is compatible with the offset beam element.

2.1. OFFSET BEAM ELEMENT

The element stiffness of the offset beam element shown in Figure 2 is formulated as follows. The displacement field is assumed as

$$u(x, z) = u_0 + (z - h/2)\psi(x), \qquad w(x, z) = w(x), \qquad \psi(x, z) = \psi(x). \tag{1}$$

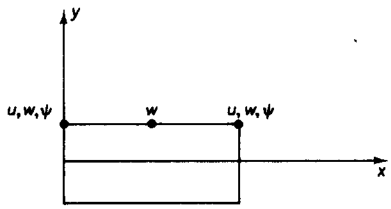

Figure 2. Offset beam element.

u_0 and ψ are defined by using linear interpolation functions,

$$u(x) = [(1 - x/L_e) \quad x/L_e][u_1 \quad u_2]^T, \qquad \psi(x) = [(1 - x/L_e) \quad x/L_e][\psi_1 \quad \psi_2]^T, \tag{2a}$$

where u_1, u_2, ψ_1 and ψ_2 are corresponding nodal displacements. w is defined by using quadratic interpolation functions,

$$w = \begin{bmatrix} (1 - 3x/L_e + 2x^2/L_e^2) \\ 4(x/L_e - x^2/L_e^2) \\ (-x/L_e + 2x^2/L_e^2) \end{bmatrix}^T \begin{Bmatrix} w_1^e \\ w_2^e \\ w_3^e \end{Bmatrix} \tag{2b}$$

where w_1^e, w_2^e and w_3^e are nodal displacements. (A list of symbols is given in the Appendix.)

Strains are derived from displacements by using the strain-displacement relations,

$$\varepsilon_{xx} = \partial u/\partial x = \partial u_0/\partial x + z\, \partial\psi/\partial x, \qquad \gamma_{xz} = \partial u/\partial z + \partial w/\partial x = \psi + \partial w/\partial x. \tag{3a, b}$$

The strain energy density is given by

$$U_0 = \tfrac{1}{2}C_{11}\varepsilon_{xx}^2 + \tfrac{1}{2}C_{55}\gamma_{xz}^2. \tag{4}$$

C_{11} and C_{55} are constants from the constitutive equations. The total strain energy in the element is given by

$$U = \int U_0 \, dv = \int_0^{L_e} \int_{-h/2}^{h/2} U_0 \, dx \, dz. \tag{5}$$

By using equations (2)-(5), the strain energy in the element can be reduced to $U = \{d_e\}^T[K_e]\{d_e\}/2$, where, $\{d_e\}$ is the vector of the elemental D.O.F., and $\{K_e\}$ is the element stiffness matrix.

The calculations involved are lengthy but straightforward and are not presented here. The consistent mass matrix is evaluated similarly from the kinetic energy of the system. This element lends itself readily to efficient analysis of such sandwich structures.

3. MODELING AND SOLUTION TECHNIQUES

As mentioned before the base structure was modeled by using the three-node shear-deformable beam element. Typically, 20 elements are used to model the beam. Very large aspect ratios are common for elements used to model the viscoelastic core. Values as high as 5000:1 have been used successfully, and are sometimes even necessary, since the viscoelastic core is only two mils thick [7]. Aspect ratios up to 200:1 were used in the present study. To validate this formulation, several calculations were made to determine natural frequencies and tip displacement of simple systems, closed form solutions to which are easily derived.

The loss factor was evaluated by using the direct frequency-response technique. In this method, a forced vibration at a known frequency is considered. System displacements are obtained by solving a system of complex-valued linear equations. The frequency-response spectrum is obtained by plotting amplitudes over a range of frequencies. The loss factor, a measure of damping, obtained from the real part of the response. This technique, although not the most efficient, was used for two reasons—simplicity and the relative small size of the problem in question.

The modeling method used is reasonably efficient. A three-layer structure is modeled with only two layers of nodes. This technique can be easily extended to two-dimensional problems. However, alternative methods for determining system loss factor will have to be used as the problem size increases [8].

4. EXPERIMENTAL PROCEDURE

The most common methods used to measure damping are the free vibration decay method, the resonant dwell method, the hysterisis loop method and the frequency-response technique. For the purpose of this research the impulse - frequency response technique was used [9]. This technique offers potential for rapid non-destructive evaluation of materials and structures. In the impulse - frequency response technique, the specimen is excited impulsively with a controlled-impact hammer which has a force transducer attached to its head. The specimen response is sensed by a non-contacting eddy current proximity probe. The signals from the force transducer and the motion transducer are fed to a Fast Fourier Transform (FFT) analyzer which displays the frequency spectrum. A block diagram of the instrumentation is shown in Figure 3. By analyzing the resonant peaks for a particular mode, the loss factor, a measure of damping, is obtained from the real part of the response spectrum, as explained in Figure 4. In this research the improved technique of Suarez and Gibson [9] was used. One of the features of this improved technique is that the excitation level is accurately controlled; therefore, the amplitude of

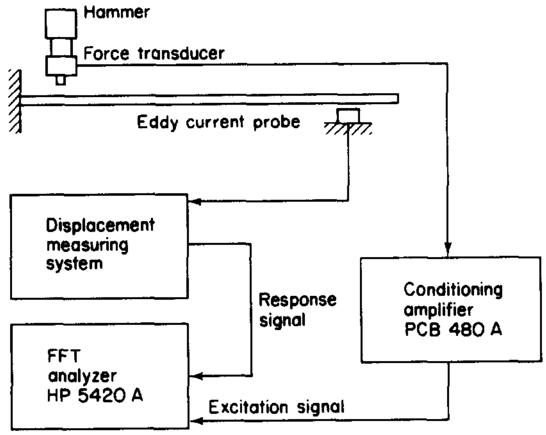

Figure 3. Flexural vibration apparatus.

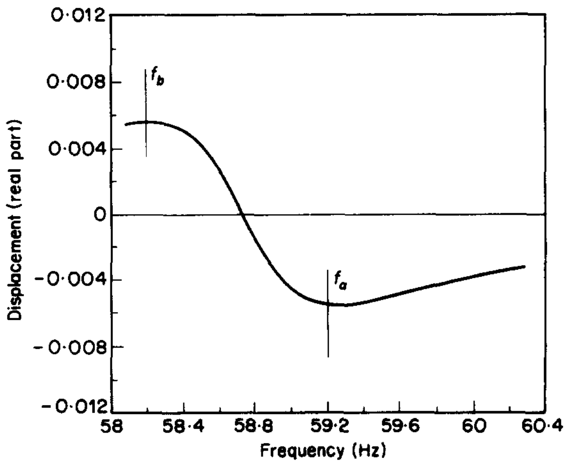

Figure 4. Real part of the response spectrum. Loss factor $= [1-(f_b/f_a)^2]/[1+(f_b/f_a)]^2$.

vibration of the specimen can be reduced to a minimum (thereby reducing air damping to a minimum). Also, the response function, which is identical in shape to the transfer function after ensemble averaging, can be used for damping measurements [9].

5. MODEL VERIFICATION

The finite element model was verified by considering a sandwich cantilever beam with a viscoelastic core. This problem has been studied extensively in previous studies [5]. Calculated resonant frequencies and system loss factors are compared with the finite element solution of Soni and Bogner [5] and a sixth order beam theory solution [10]. The geometry of the beam is shown in Figure 5. For the purpose of comparison, a hypothetical damping material with frequency and temperature invariant properties, similar to the one considered by Soni [5], is used. The material properties of the sandwich beam are given in Table 1.

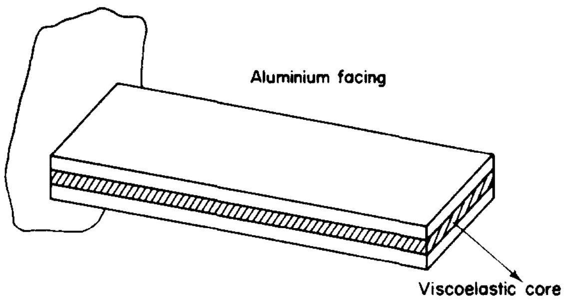

Figure 5. Sandwich beam. Length 177·8 mm, width 25·4 mm.

TABLE 1

Material properties for sandwich beam

	Aluminum	Viscoelastic core
Thickness (mm)	1·524	0·127
Young's modulus (GPa)	69	0·0021
Poisson ratio	0·3	0·499
Loss factor		1·0
Specific gravity	2·8	0·97

The damped frequencies and corresponding modal loss factors from the present finite element analysis are compared with those from previous analyses [5] in Table 2. The values of the damped resonant frequencies and the system loss factors are in good agreement. In the present model, a total of 80 active degrees of freedom was used to model the sandwich beam; Soni and Bogner employed 440 active degrees of freedom in their model. The direct frequency-response method explained earlier was used to calculate modal damping.

TABLE 2

Model comparison

	Loss factor			Frequency (Hz)		
	Present	6th order	Soni	Present	6th order	Soni
Mode 1	0·1997	0·2022	0·2019	67·5	67·4	67·4
Mode 2	0·2117	0·2177	0·2180	298·1	302·8	307·0
Mode 3	0·1452	0·1502	0·1500	752·8	748·6	762·0

6. RESULTS AND DISCUSSION

Two different materials are considered for the purpose of analysis. Material 1 is a hypothetical material with low modulus and high loss factor typical of off-axis composites. Typical glass-epoxy data was used for material 2. The material properties of material 1, glass-epoxy and the soft aluminum constraining layer are given in Table 3. For all cases, the damping tape used was 3M's SJ2052x, a class of constrained viscoelastic damping tape. For this tape, the viscoelastic layer and the aluminum constraining layer are 0·127 mm and 0·254 mm thick respectively. The shear modulus and loss factor of the damping material, as a function of temperature and frequency, can be found in reference [11].

TABLE 3

Material properties

	Material 1	Material 2	Constraining layer
V_f (%)	50	50	—
ρ (g/cm^3)	1·90	1·90	2·76
E_L (GPa)	28	36	69
E_T (GPa)	8·8	8·8	69
G_{LT} (GPa)	3	3	26
ν_{LT}	0·28	0·28	0·32
η_L	0·01	0·004	0·005
η_T	0·015	0·01	0·005

Structural damping with and without add-on viscoelastic layer damping was evaluated analytically and experimentally for material 2. Results of the effects of different parameters such as the quantity of treatment and the location of the treatment on the overall damping of the system are presented. Three different unidirectional composite specimens were tested, and the average measured loss factor was used as input data to the finite element model. The same specimens were also tested after application of the damping treatment. Each specimen was 203 mm long and 3·6 mm thick.

In Figure 6 is shown the magnitude of the response as a function of the frequency of the forced vibration for three different lengths of treatment for material 1. The change in system response due to addition of the viscoelastic material can be seen from the figure.

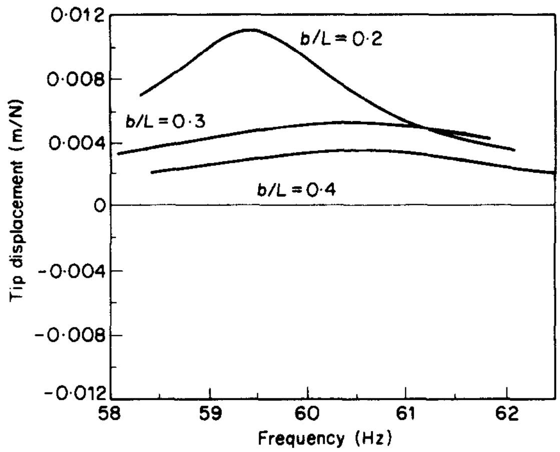

Figure 6. Response spectra for different lengths of treatment. Material 1, $a/L=0$.

Displacement is plotted in meters, per Newton of applied force. Large reductions in response amplitude can be seen due to application of the damping tape.

The variation of loss factor with tape length for material 1 is shown in Figure 7. For mode 1, the loss factor increases rapidly from $b/L=0$ to $b/L=0{\cdot}6$, after which it shows a slight drop. The existence of a tape length, b, for which $b/L<1$ and damping is optimal

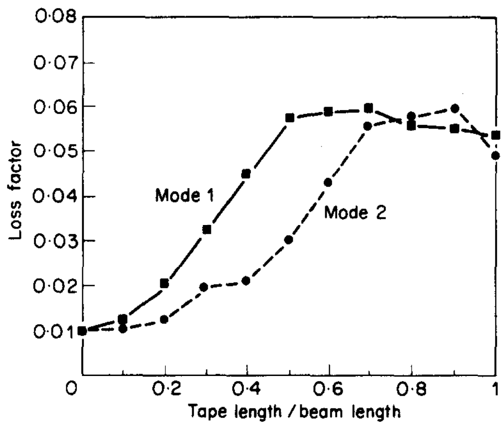

Figure 7. Variation of loss factor. Material 1, $a/L=0$.

is significant. This result shows that shear deformation of the viscoelastic core is the primary source for energy dissipation. For lengths greater than the optimal value, the deformation of the viscoelastic core follows the extensional deformation of the surface of the beam. The trend observed for mode 2 is different from that for mode 1. While treatment closer to the root of the beam seems to have the greatest effect on mode 1, the center of the beam seems to be the optimal location for mode 2. This suggests that application of damping material to the points of high strain energy density yields best results. These results are also evident from Figures 8 and 9 which show the variation of system loss factor with tape length, for different locations of the damping treatment for mode 1 and mode 2 respectively.

The analytical and experimental results for the $[0]_{16}$ glass–epoxy laminate (material 2) are presented in Figure 10. Good agreement between the data is seen for both mode 1

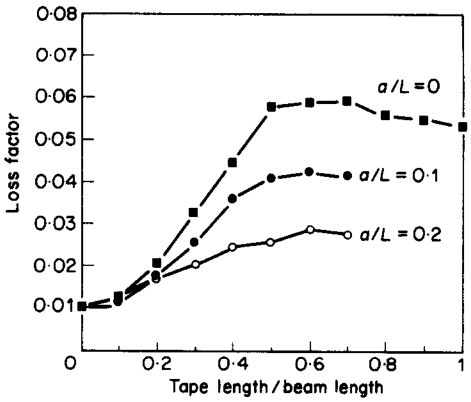

Figure 8. Effects of location on loss factor (material 1, mode 1).

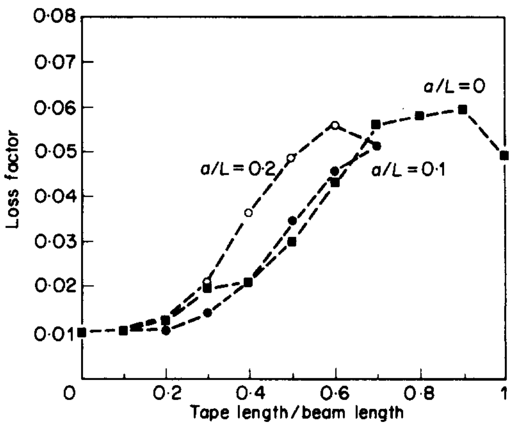

Figure 9. Effects of location on loss factor (material 1, mode 2).

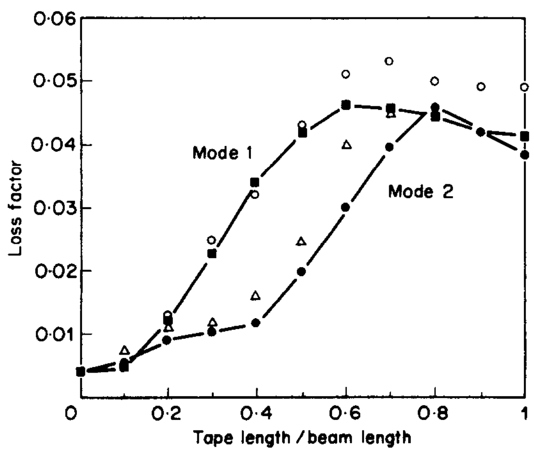

Figure 10. Analytical and experimental results for material 2; $a/L = 0{\cdot}0$. Experimental results: ○, mode 1; △, mode 2.

and mode 2. Analytical and experimental results project similar system behavior for varying amounts of damping treatment. The loss factor of the base structure is small for material 2 as compared to material 1. However, the change in system loss factor with the application of damping tape for both systems is about the same. For material 2, neglecting the base structure loss factors would yield reasonable results for system response, but for material 1 (as is true for most composite materials) the base structure loss factor cannot be neglected.

The variation of tip displacement at resonance with amount of treatment for materials 1 and 2 is shown in Figures 11-14. For both materials the vibration amplitude is seen to reduce dramatically with increasing amounts of damping treatment. As can be seen from the damping curves, the presence of an optimal length and location for a given structure and loading condition is evident. It can also be seen that treatment closer to the root of the beam will have a stronger influence on system response for mode 1, while treatment located away from the root of the beam has a stronger influence on mode 2 response. Several other factors, such as the thickness of the damping layer and the type of damping treatment, also affect the system response strongly.

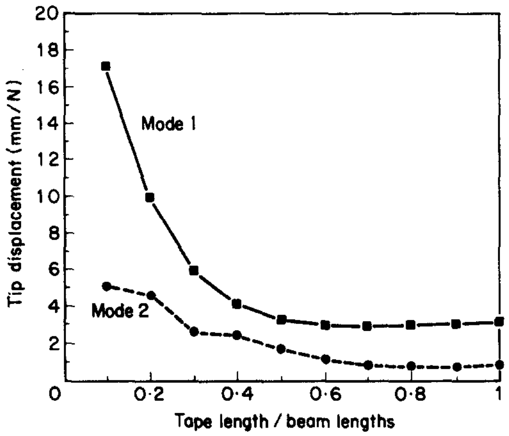

Figure 11. Variation of tip displacement; material 1, $a/L=0{\cdot}0$.

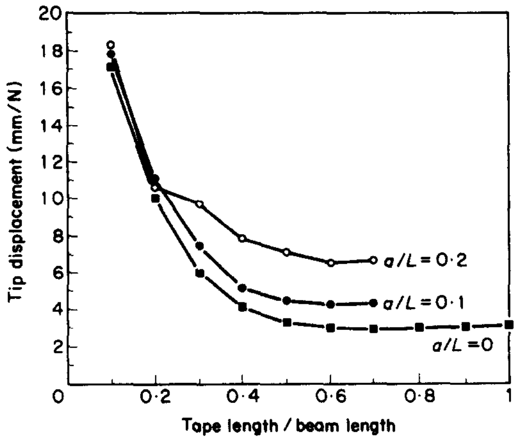

Figure 12. Effect of location on tip displacement; material 1, mode 1.

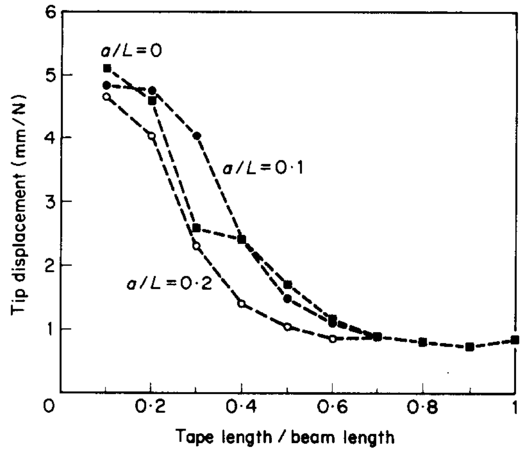

Figure 13. Effect of location on tip diaplacement; material 1, mode 2.

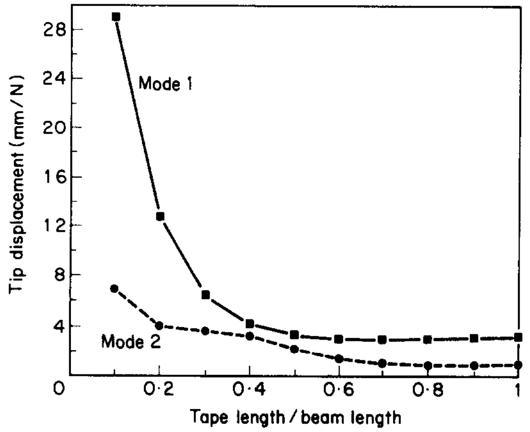

Figure 14. Variation of tip displacement; material 2, $a/L=0{\cdot}0$.

7. CONCLUDING REMARKS

On the basis of the numerical and experimental results presented, it is seen that the finite element model presented is an accurate and efficient representation of a sandwich beam and that viscoelastic surface layer treatments can be used to improve significantly the dynamic response of structures. Increases in overall system damping and large reductions in response amplitudes are achieved by using damping treatment. Results also show, for each mode of vibration, that there exists a length, location and a thickness of the damping tape, for a given thickness of the constraining layer, for which the overall system damping is maximized.

In future the work will be extended to accommodate the effects of continuous variation in cross-section (this is already possible with a little modification), pre-stress, initial twisting and rotation on the system response.

ACKNOWLEDGMENT

This work is sponsored by the Army Research Office and monitored by Dr Gary L. Anderson under contract No. DAAL03-88-k0013.

REFERENCES

1. A. D. NASHIF, D. I. G. JONES and J. P. HENDERSON 1985 *Vibration Damping*. New York: John Wiley.
2. D. ROSS, E. E. UNGAR and E. M. KERWIN, JR 1959 *ASME Monograph on Structural Damping section* 3. Damping of plate flexural vibrations by means of viscoelastic laminae.
3. R. PLUNKETT and C. T. LEE 1970 *Journal of the Acoustical Society of America* **48**, 151-158. Length optimization for constrained viscoelastic layer damping.
4. C. D. JOHNSON and D. A. KIENHOLZ 1982 *American Institute of Aeronautics and Astronautics Journal* **20**(9), 1264-1290. Finite element prediction of damping layers.
5. N. L. SONI and F. K. BOGNER 1982 *American Institute of Aeronautics and Astronautics Journal* **20**(5), 700-707. Finite element vibration analysis of damped structures.
6. M. L. SONI 1981 *Shock and Vibration Bulletin* **51**. Finite element analysis of viscoelastically damped sandwich structures.
7. C. D. JOHNSON, D. A. KIENHOLZ, E. M. AUSTIN and N. E. SCHNEIDER 1984 *Proceedings of the Vibration Damping Workshop* 27-29 *February* 1984, HH1-HH8. Finite element design of viscoelastically damped structures.
8. R. A. BROCKMAN 1984 *Proceedings of the Vibration Damping Workshop* 27-29 *February* 1984. On vibration damping analysis using the finite element method.
9. S. A. SUAREZ and R. F. GIBSON 1987 *Journal of Testing and Evaluation* **15**(2), 114-121. Improved impulse-frequency response techniques for measurements of dynamic mechanical properties of composite materials.
10. D. K. RAO 1978 *Journal of Mechanical Engineering Science* **20**, 271-282. Frequency and loss factors of sandwich beams under various boundary conditions.
11. M. L. DRAKE 1980 *Technical Report AFWAL-TR*-80-4093. Polymeric material testing procedures to determine damping properties and the results of selected commercial material.

APPENDIX: LIST OF SYMBOLS

a	distance of damping tape from support
b	length of treatment
d_e	vector of elemental degrees of freedom
E	extensional modulus
G	shear modulus
GPa	giga pascal
h	thickness
Hz	Hertz
K	stiffness matrix
L	length
M	mass matrix
Psi	pounds per square inch
u	extensional displacement
U	strain energy
V_f	fiber volume fraction
w	deflection
γ	shear strain
ε	extensional strain
η	loss factor
ν	Poisson ratio
ρ	density
σ	normal stress
τ	shear stress
ψ	rotation
ω	frequency